HHS Public Access

Author manuscript

Exp Dermatol. Author manuscript; available in PMC 2017 September 01.

Published in final edited form as:

Exp Dermatol. 2016 September ; 25(9): 688–693. doi:10.1111/exd.13034.

Comparison of the acute ultraviolet photoresponse in congenic albino hairless C57BL/6J mice relative to outbred SKH1 hairless mice

Raymond L. Konger[1,2], **Ethel Derr-Yellin**[1], **Delaram Hojati**[1], **Cathleen Lutz**[3], and **John P. Sundberg**[4]

[1]Department of Pathology & Laboratory Medicine, Indiana University School of Medicine, Indianapolis, IN

[2]Department of Dermatology, Indiana University School of Medicine, Indianapolis, IN

[3]Rare and Orphan Disease Center, Department of Genetic Resources Sciences, The Jackson Laboratory, Bar Harbor ME

[4]Research and Development, The Jackson Laboratory, Bar Harbor, ME

Abstract

Hairless albino Crl:SKH1-*Hr*^{hr} mice are commonly utilized for studies in which hair or pigmentation would introduce an impediment to observational studies. Being an outbred strain, the SKH1 model suffers from key limitations that are not seen with congenic mouse strains. Inbred and congenic C57BL/6J mice are commonly utilized for modified genetic mouse models. We compare the acute UV-induced photoresponse between outbred SKH1 mice and an immune competent, hairless, albino C57BL/6J congenic mouse line [B6.*Cg-Tyr*$^{c\text{-}2J}$ *Hr*^{hr}/J]. Histologically, B6.*Cg-Tyr*$^{c\text{-}2J}$ *Hr*^{hr}/J skin is indistinguishable from that of SKH1 mice. The skin of both SKH1 and B6.*Cg-Tyr*$^{c\text{-}2J}$ *Hr*^{hr}/J mice exhibited a reduction in hypodermal adipose tissue, the presence of utricles and dermal cystic structures, the presence of dermal granulomas, and epidermal thickening. In response to a single 1500 J/m^2 UVB dose, the edema and apoptotic response was equivalent in both mouse strains. However, B6.*Cg-Tyr*$^{c\text{-}2J}$ *Hr*^{hr}/J mice exhibited a more robust delayed sunburn reaction, with an increase in epidermal erosion, scab formation, and myeloperoxidase activity relative to SKH1 mice. Compared with SKH1 mice, B6.*Cg-Tyr*$^{c\text{-}2J}$ *Hr*^{hr}/J also exhibited an aberrant proliferative response to this single UV exposure. Epidermal Ki67 immunopositivity was significantly suppressed in B6.*Cg-Tyr*$^{c\text{-}2J}$ *Hr*^{hr}/J mice at 24 hours post-UV. A smaller non-significant reduction in Ki67 labeling was observed in SKH1 mice. Finally, at 72 hours post-UV, SKH1 mice, but not B6.*Cg-Tyr*$^{c\text{-}2J}$ *Hr*^{hr}/J mice, exhibited a

Corresponding authors: Questions concerning the UV responses of the mice should be directed to Raymond L. Konger, MD. Associate Professor of Pathology and Laboratory Medicine and Dermatology. Indiana University School of Medicine, 975 W. Walnut Street, IB424F, Indianapolis, IN 46202, USA. Telephone: (317) 274-4154. rkonger@iupui.edu. Questions concerning the breeding and background genetics of B6.*Cg-Tyr*$^{c\text{-}2J}$ *Hr*^{hr}/J mice should be directed to John P. Sundberg, DVM, PhD. Professor, The Jackson Laboratory, 600 Main Street, Bar Harbor, Maine 04609, USA. Telephone: 207-288-6410. john.sundberg@jax.org.

CONFLICT OF INTERESTS

JPS and CL are employed by The Jackson Laboratory, which offers the B6.*Cg-Tyr*$^{c\text{-}2J}$ *Hr*^{hr}/J mice for sale to the research community. JPS has a research contract with the Medicinal Bioconvergence Research Center (Biocon) for preclinical trials unrelated to this work. Otherwise, the authors have no conflicts of interest.

significant increase in Ki67 immunolabeling relative to non-irradiated controls. Thus, B6.*Cg-Tyr*$^{c\text{-}2J}$ *Hr*^{hr}/J mice are suitable for photobiology experiments.

Keywords

Photobiology; Animal model; Hairless; Albino; Congenic

Introduction

Hairless mice that also carry an albino mutation (tyrosinase) are ideally suited for studies examining cutaneous environmental or toxicological exposures and wound healing studies. While hair removal can be performed by shaving, depilatory chemical agents, or waxing, all of these procedures produce variability due to chemical or physical tissue damage and resulting inflammatory responses [1]. In addition, melanosome synthesis in mice occurs nearly exclusively in the hair follicles during the growth or anagen phase of the hair cycle [2]. In adult mouse hair growth cycling occurs as various sized patches of synchronized hair follicle development [3]. Since melanin absorbs ultraviolet (UV) light, the patches of melanin production introduce significant variability into photobiological studies even in shaved mice. Moreover, hairless mice exhibit greater sensitivity to cutaneous chemical and UV-induced carcinogenesis relative to shaved controls [4]. Tumors derived from hairless mice also better represent human skin cancer, with a squamous cell carcinomas and papilosquamous tumors predominating in hairless mice, while shaved mice develop primarily fibrosarcomas that are infrequent in humans [5].

Due to the absence of congenic strains, outbred SKH1 hairless, albino mice are frequently utilized for photobiology studies [1, 6–9]. For studies that utilize genetically modified mice to address gene specific effects, genetic background variability is reduced by extensive backcrossing of transgenic or knockout mice into the SKH1 background [10–14]. However, the genetic background variability of non-congenic SKH1 mice introduces uncertainty when assessing the role of a specific gene in a pathological or physiological process. While inbred SKH1 mice (SKHIN/Sprd) have been produced, the generation of transgenic progeny by standard pronuclear microinjection occurs at low efficiency [15]. Moreover, tumor cell lines derived from SKHIN/Sprd are not available for syngeneic tumor transplantation studies.

Albino C57BL/6J (C57BL/6J-*Tyr*$^{c\text{-}2J}$) mice are derived from C57BL/6J mice harboring a spontaneous point mutation in the tyrosinase gene resulting in the inability of melanocytes to metabolize tyrosine to dopaquinone, which is required for the subsequent production of melanin [16]. Loss of melanin production leads to the albino phenotype, which is a relatively common autosomal recessive trait in mice (204 allelic mutations are listed in Mouse Genome Informatics, 23 March 2016). The albino trait is also helpful to minimize variability in photobiology and toxicological studies due to pigment.

While melanocytes are concentrated in hair follicles in mice, pigmented hairless mice still exhibit increased pigmentation following exposure to carcinogens such as dimethylbenzanthracene and ultraviolet B (UVB) [17, 18]. Thus, photobiological studies are generally carried out in both hairless and albino mice to reduce experimental variability.

Moreover, intravital imaging studies are best accomplished in hairless, albino mouse skin [19–21].

The hairless gene (*HR* in humans, *Hr* in mice; HR for the protein in both species) encodes a nucleoprotein that is highly expressed in the skin and brain [22]. HR acts as a transcriptional co-repressor for nuclear receptors, including the Vitamin D receptor (VDR), thyroid hormone receptor (TR), and retinoic acid-like orphan receptor alpha (RORA) [1, 23–25]. In addition, the hairless protein exhibits histone demethylase activity [22, 25]. This suggests that HR may interact with a number of different signaling pathways [25]. In both humans and mice, hairless is essential for re-entry into the anagen or growth phase of hair follicles [24]. In humans, homozygosity for mutations of the hairless (*HR*) gene are associated with rare congenital atrichias or hypotrichosis, as well as the formation of papular cysts [26–28]. Mutations at various sites resulting in reduced *Hr* gene expression have been described in mice, resulting in hairless phenotype (Hr^{hr}). Mutations causing greater loss of *Hr* expression result a more severe phenotype characterized by both hairlessness and excessive wrinkling or skin folds (rhinoceros or rhino mice; Hr^{rh}) [29].

Following an acute exposure to UVB light, SKH1 mice exhibit a characteristic response that resembles the human sunburn reaction [13]. Over the first 24 hours, the initial cutaneous photoresponse is marked by increased vasopermeability resulting in increased edema, an initial increase in inflammatory cell infiltration, and increases in skin thickness. Given that UVB directly damages DNA through photochemical reactions, while UVA indirectly damages DNA through oxidative stress, the initial epidermal photoresponse is marked by the DNA damage response, including a UV dose-dependent increase in apoptotic keratinocytes and a marked exit of cells from the cell cycle to allow for DNA repair [30]. After the initial 24 hour period, there is a gradual increase in acute inflammatory cell infiltration along with a shift in keratinocytes from the DNA damage repair and apoptotic responses to a surge in keratinocyte proliferation. This is most prominent within the first 72 hours following UV treatment and serves to repopulate the epidermis and its normal epidermal permeability barrier function. In addition, the resulting hyperplastic response may also serve an adaptive role to increase the optical thickness and decrease subsequent UV penetration and DNA damage to the proliferative basal cell niche of the epidermis [31]. In this study, we sought to determine the acute photoresponse in hairless, albino C57BL/6J mice, and to compare this response to the widely used outbred SKH1 mouse model.

Results

Comparative histology of the skin of C57BL/6J homozygous for both the hairless allele and lacking tyrosinase (B6.*Cg-Tyr*$^{c\text{-}2J}$ *Hr*^{hr}/J) and SKH1 mice

By visual inspection, the skin of SKH1 and B6.*Cg-Tyr*$^{c\text{-}2J}$ Hr^{hr}/J mice are not observably different (Fig 1A & B). We therefore examined the skin of both strains histologically. Mice homozygous for the *Hr* allele are known to exhibit a decrease in whole body and subcutaneous adipose tissue [23, 32]. It is also known that the hypodermal fat layer in mice undergoes changes in thickness during the hair cycle, being thickest during telogen and thinnest during anagen [33]. We therefore measured the thickness of the hypodermis in the skin of both hairless mouse strains as well as in C57BL/6J mouse skin during both anagen

and telogen (Fig 1C). As expected, both SKH1 and B6.*Cg-Tyr*$^{c\text{-}2J}$ *Hr*^{hr}/J mice exhibit a reduction in the thickness of the hypodermal fat layer relative to wildtype C57BL/6J mice, regardless of whether the mouse skin was in either telogen or anagen phase. Also as expected, wildtype C57BL/6J mice exhibited a significant increase in the hypodermal thickness during anagen relative to the telogen phase of the hair cycle. The skin of B6.*Cg-Tyr*$^{c\text{-}2J}$ *Hr*^{hr}/J mice also exhibited the characteristic structures that are observed in other hairless mouse skin [1]. This includes utricules, cornified dermal cysts, and dermal granulomas (Fig 1D–F).

SKH1 and B6.*Cg-Tyr*$^{c\text{-}2J}$ *Hr*^{hr}/J mice exhibit similar edema reactions to identical UVB treatments

In mice, the initial acute vascular response to UVB is primarily that of vascular permeability and edema that is detected as an increase in skin thickness measurements at 24 and 72 hours post UVB [35, 36]. Thus, it was not surprising that there was no visual evidence of an erythema reaction in either SKH1 or B6.*Cg-Tyr*$^{c\text{-}2J}$ *Hr*^{hr}/J mice at 24 hours post-UVB (not shown). We therefore examined the edema response to an acute UVB treatment. In Fig 2A, there is no significant difference in basal skin thickness measurements between non-UVB treated SKH1 mice, C57BL/6J mice, and B6.*Cg-Tyr*$^{c\text{-}2J}$ *Hr*^{hr}/J mice (mean and SD of 0.743 ± 0.097; 0.728 ± 0.029; and 0.736 ± 0.112 mm, respectively). UVB induced a similar pattern of edema response in both SKH1 mice and B6.*Cg-Tyr*$^{c\text{-}2J}$ *Hr*^{hr}/J mice as evidenced by a significant increase in skin thickness measurements at 24 and 72 hours (Fig 2A). In Figs 2B–G, the edema response is seen histologically as an expansion of the dermis and hypodermis at 24 and 72 hours after UVB treatment that was accompanied by inflammatory cell infiltrates. Epidermal hyperplasia was also noted at 72 hours (Figs 2D & G).

B6.*Cg-Tyr*$^{c\text{-}2J}$ *Hr*^{hr}/J and SKH1 mice exhibit similar apoptotic responses to an acute UV treatment

UVB-induced DNA damage promotes an apoptotic response in mouse skin that that is observed at 24 hours post-UVB, but not at 72 hours post-UVB [36]. We next examined the apoptotic response by counting epidermal cells staining positive for both activated caspase 3 (CASP3$^+$) and pan-cytokeratin (pan-CK$^+$) by immunofluorescence (Fig 2H & Supplemental Fig 1). As with the skin thickness changes, SKH1 and B6.*Cg-Tyr*$^{c\text{-}2J}$ *Hr*^{hr}/J mice exhibited similar patterns of UV-induced cytotoxicity with an elevation of Pan-CK$^+$/CASP3$^+$ cells at 24 hours and a reduction at 72 hours (Fig 2H). In Supplemental Fig 1, the increase in Casp3$^+$ cells within the epidermis of both mouse strains is readily evident at 24 hours, while the decrease in epidermal Casp3$^+$ cells seen at 72 hours corresponds to readily apparent epidermal hyperplasia. B6.*Cg-Tyr*$^{c\text{-}2J}$ *Hr*^{hr}/J and SKH1 mice also exhibited a typical UVB-induced epidermal cytotoxic response by histologic assessment when examined 24 hours after UVB treatment (Fig 2I & J). This was seen by marked epidermal disruption, spongiosis, and the presence of multiple apoptotic cells.

Relative to SKH1 mice, B6.*Cg-Tyr^{c-2J} Hr^{hr}*/J mice exhibit a more pronounced sunburn reaction at 72 hours post-UVB that is seen as increased epidermal disruption, scab formation and leukocyte infiltration

UVB-induced inflammation and overlying epidermal proliferation peak at approximately 72 hours after UVB treatment in SKH1 mice [13]. When compared with non-UVB treated mice, both SKH1 and B6.*Cg-Tyr^{c-2J} Hr^{hr}*/J mice exhibited a visible sunburn reaction at 72 hours post-UVB treatment (Figs 3A & C). This reaction was characterized by erythema, epidermal peeling, and scab formation. While scab formation was modest in SKH1 mice, significantly greater scab formation occurred in B6.*Cg-Tyr^{c-2J} Hr^{hr}*/J mice (Figs 3B, D, and E). This marked increase in scab formation at 72 hours was accompanied by a significant increase in leukocyte myeloperoxidase (MPO) activity in the B6.*Cg-Tyr^{c-2J} Hr^{hr}*/J mice relative to SKH1 mice (Fig 3F). This increase in MPO activity is likely attributable to the large numbers of inflammatory cells present in the overlying scabs, indicating the scabs were formed from a purulent exudative process (Fig 3D & Supplemental Fig 2A). In contrast, dermal accumulation of inflammatory cells in areas of skin with no scab formation did not appear to be significantly different (Figs 2D & G and Supplemental Figs 2C & D). This suggests that the increase in myeloperoxidase levels were accounted by the marked increase in purulent exudate that is driven by loss of the epidermal permeability barrier.

The proliferative response to UVB treatment is altered in B6.*Cg-Tyr^{c-2J} Hr^{hr}*/J mice relative to SKH1 mice

UVB damaged cells undergo growth arrest during DNA repair. This is consistent with the decrease in expression of the proliferative marker Ki67 in both B6.*Cg-Tyr^{c-2J} Hr^{hr}*/J mice and SKH1 mice when examined 24 hours after UVB treatment (Figs 4A – C). In non-irradiated controls for both B6.*Cg-Tyr^{c-2J} Hr^{hr}*/J and SKH1 mice, Ki67^{+} cells were scattered in the basal layer of both the interfollicular and follicular epidermis (Figs 4B & C). In both mouse lines, Ki67^{+} cells were absent in the basal layer of the interfollicular epidermis 24 hours after UVB (Figs 4B & C). However, positive cells were found in the deeper portions of the follicular utricules and the ductal lining cells of sebaceous glands (Figs 4B & C). Relative to the suppression in Ki67 immunolabeling seen at 24 hours after UVB, a significant rebound in Ki67^{+} epidermal cells was observed in both B6.*Cg-Tyr^{c-2J} Hr^{hr}*/J and SKH1 mice at 72 hours post UVB treatment (Figs 4A–C). However, this rebound was not as pronounced in B6.*Cg-Tyr^{c-2J} Hr^{hr}*/J mice as the Ki67^{+} labeling at 72 hours was significantly lower than that observed in SKH-1 mice (Fig 4A). Moreover, while Ki67^{+} cells were significantly increased at 72 hours relative to non-irradiated control SKH1 mice, there was no significant difference in Ki67^{+} immunolabeling in B6.*Cg-Tyr^{c-2J} Hr^{hr}*/J mice when the 72 hour time point was compared with non-irradiated controls (Fig 4A). It should be noted that the large areas of epidermal erosion in the B6.*Cg-Tyr^{c-2J} Hr^{hr}*/J mice likely impacted these findings, as intact areas appeared to exhibit similar hyperplastic changes (Figs 2D & G, 4B & C and Supplemental Fig 1). However, even in areas of non-eroded hyperplastic epidermis, there appeared to be an increase in Ki67 immunolabeling in SKH1 mice relative to B6.*Cg-Tyr^{c-2J} Hr^{hr}*/J mice (Figs 4B & C).

Discussion

The lack of hair and pigmentation seen in SKH1 mice has led to their widespread use for photobiology and photocarcinogenesis studies. However, a major disadvantage of this mouse model is that these mice are outbred. Genetically modified mice are frequently generated in inbred or congenic C57BL/6 mice. Having a B6 congenic strain carrying the Hr^{hr} allele that lacks pigmentation provides a much needed tool to investigate the genetic influences on UVB light induced skin disease and cancer. Thus, we characterized the UVB photoresponse of a hairless and albino C57BL/6 congenic mouse strain and compared this response to that observed in SKH1 mice. We show that relative to C57BL/6 mice, the skin of both B6.*Cg-Tyr^{c-2J} Hr^{hr}*/J and SKH1 mice are similar, both grossly and by microscopic exam. We also show that the acute photobiological response of B6.*Cg-Tyr^{c-2J} Hr^{hr}*/J and SKH1 mice are similar in some, but not all, respects.

In humans, the acute vascular response to UV treatment results in a significant early vasodilation and measureable erythema response (sunburn) within the first 24 hours [34]. This sunburn reaction differs markedly for different individuals at a given UVB dose. Thus, the minimal erythemal dose (MED) in humans is utilized in studies to tailor UVB doses to account for individual susceptibility to the sunburn reaction. In mice, little or no erythema response is seen at 24 hours for doses that induce a pronounced edematogenic dose. Therefore, the minimal edematogenic dose (MED) is utilized in mice and is defined as the UVB dose that produces a minimal edema response at 24 hours following treatment [35, 37]. In SKH1 mice, the MED has been reported to be from 900 – 2240 J/m^2 UVB [1, 30]. Following treatment with a single dose of 1500 J/m^2 UVB, the edema response at 24 hours post treatment was not significantly different between the SKH1 and B6.*Cg-Tyr^{c-2J} Hr^{hr}*/J mice. In addition, both B6.*Cg-Tyr^{c-2J} Hr^{hr}*/J and SKH1 mice exhibited a similar temporal pattern of UVB-induced activated caspase 3, suggesting that the apoptotic response is very similar in both strains of mice. Thus, based on this criteria alone, there does not appear to be a significant difference in the MED for B6.*Cg-Tyr^{c-2J} Hr^{hr}*/J and SKH1 mice.

In contrast to the early UVB-induced changes observed at 24 hours, B6.*Cg-Tyr^{c-2J} Hr^{hr}*/J mice exhibit a more pronounced sunburn response at 72 hours post-UVB irradiation. Large areas of epidermal erosion leading to inflammatory exudates and scab formation were observed in B6.*Cg-Tyr^{c-2J} Hr^{hr}*/J mice that were minimally present in SKH1 mice. Thus, the markedly dissimilar sunburn response seen at 72 hours between SKH1 mice and the congenic B6.*Cg-Tyr^{c-2J} Hr^{hr}*/J mice suggests that the mouse MED correlates poorly with the overall sunburn response. This raises doubts that the edematogenic response seen a 24 hours post-UVB treatment is the appropriate response to assess for mouse photobiology studies. Given that the human and mouse MEDs measure different responses, it is perhaps not surprising that a poor correlation exists between human and mouse MEDs: while the MED in albino SKH1 mice is reported to be 900 J/m^2 and greater, the average MED is 148 J/m^2 in highly sunburn-prone individuals (Fitzpatrick scale I) [38]. Thus, the UVB dose that we utilized for our studies (1500 J/m^2) would correspond to roughly 10 times that of the MED in light-skinned humans. Interestingly, the relevance of the mouse MED has previously been questioned, as the MED fails to correlate well with the carcinogenic activity of a UV light source [37]. Certainly, our studies suggest that it would be prudent to utilize lower UVB

doses for photobiological experiments in B6.*Cg-Tyr*$^{c\text{-}2J}$ *Hr*^{hr}/J mice to reduce animal distress under the principle of Refinement. These studies also suggest that sunburn reactions at 72 hours (erythemal reaction or epidermal erosion) may prove more useful for establishing pathologically relevant UVB doses in mice.

The mechanisms for the more robust sunburn reaction that we observed in B6.*Cg-Tyr*$^{c\text{-}2J}$ *Hr*^{hr}/J mice relative to SKH1 mice at 72 hours post-UVB treatment are unclear. As noted above, there were no significant differences in the edema or apoptotic response that was observed at 24 hrs post-UVB. Given that the release of inflammatory mediators and the apoptotic response can be tied to the initial DNA damage response, this data does not suggest that B6.*Cg-Tyr*$^{c\text{-}2J}$ *Hr*^{hr}/J mice are prone to increased DNA damage or a major disruption of the DNA damage response. However, it must be noted that our apoptosis data is limited to 24 and 72 hours, thus, it is possible that the apoptotic response is greater in B6.*Cg-Tyr*$^{c\text{-}2J}$ *Hr*^{hr}/J mice at other time points. It is also possible that the original derivation of SKH1 mice from a non-congenic background resulted in selective pressure for the adoption of more UVB resistant traits that are independent of the *Hr* and *Tyr* genes. These can be identified in the future by quantitative trait locus analysis followed by genetic manipulation of candidate genes using existing mutant mice on a B6 background or using CRISPR technology.

At 72 hours post-UVB, SKH1 mice exhibited a significant increase in Ki67 immunolabeling relative non-UVB treated epidermis. In contrast, this delayed proliferative response was significantly blunted in B6.*Cg-Tyr*$^{c\text{-}2J}$ *Hr*^{hr}/J mice. This blunted response correlates with the marked epidermal barrier disruption and scab formation seen in the congenic mouse line. Epidermal hyperplasia is thought to be necessary to provide a thickened optical barrier to subsequent UVB exposures [31]. This is important, as UVB-induced mutations within the proliferative basal layer of the epidermis are key to forming initiating mutations that can lead to neoplastic disease [39]. Moreover, the proliferative response is necessary to replace apoptotic cells within the epidermis. Failure to replace these dead cells efficiently could lead to a prolonged barrier disruption, with resulting fluid loss and increased entry of environmental pathogens. Thus, it is interesting that SKH1 mice exhibited a more robust hyperplastic response to UVB treatment relative to B6.*Cg-Tyr*$^{c\text{-}2J}$ *Hr*^{hr}/J mice. It is possible that the more robust delayed proliferative response seen in SKH1 mice represents an example of the natural selection of a UVB resistant trait that is less established in B6.*Cg-Tyr*$^{c\text{-}2J}$ *Hr*^{hr}/J mice. While we cannot rule out a greater degree of epidermal proliferation at other time points besides the 72 hour time point examined in this study, the greater degree of epidermal disruption and scab formation do not suggest that a further delay in the proliferative response would provide a greater selective advantage.

In conclusion, we present a congenic hairless, albino C57BL/6 mouse model that is suitable for generating transgenic mice with a clean genetic background to assess genetic influences on photobiology or toxicology. Indeed, the differences in the sunburn and proliferative responses that we found between the two strains highlights the impact of the genetic background on the photoresponse.

Methods

Animals

The B6.albino; hairless mice B6.Cg-*Tyr*$^{c\text{-}2J}$ *Hr*^{hr}/J, (JAX stock # 017840) was constructed at The Jackson Laboratory by mating C57BL/6J-albino mice (Stock No. 000058) with C57BL/6-hairless mice (also segregating for *H2-T18*^{a}; Stock No. 001737). The B6.albino; hairless colony was then maintained by breeding females homozygous for the albino mutation and heterozygous for the hairless mutation with males homozygous for the albino mutation and homozygous for the hairless mutation. During the first few rounds of breeding, animals were screened and selected to replace the *H2-T18*^{a} allele with the respective C57BL/6J allele (*H2-T18*^{b}). Hairless, albino SKH1 mice were purchased from Charles Rivers Laboratories (Crl:SKH1-*Hr*^{hr}; Wilmington, MA; referred to as SKH1 mice throughout the manuscript). While SKH1 mice do not exhibit breeding issues, female B6.*Cg-Tyr*$^{c\text{-}2J}$ *Hr*^{hr}/J mice homozygous for the mutated *Hr* allele are fertile, but exhibit poor nursing behavior resulting in reduced or absent litter. Similar breeding issues have been described for HRS/J-*Hr*$^{hr/hr}$ mice [40], the strain from which the *Hr*^{hr} allele was obtained from to create the B6.Cg-*Hr*^{hr}/J congenic strain. All mouse studies were approved by the Indiana University-Purdue University at Indianapolis Animal Care and Use Committee.

UVB treatments

Mice were first immobilized by intraperitoneal (ip) injection with Ketamine / Xylazine, then irradiated with 1500 J/m^2 of UVB using a bank of two Westinghouse FS40 sunlamps (National Biological Corp., Twinsberg, OH) as previously described [13].

Statistical analysis

Data was plotted using GraphPad Prism 5.0 software using a statistical significance cutoff of $p < 0.05$.

Remaining Methods can be found in Supplemental Material

Supplementary Material

Refer to Web version on PubMed Central for supplementary material.

Acknowledgments

This work was supported in part through National Institutes of Health (NIH) funding from the National Institute of Environmental Health Sciences (NIEHS), ES020965 (RLK) and National Institute of Arthritis, Musculoskeletal, and Skin Diseases (NIAMS), AR063781 (JPS). RLK and JPS conceived and designed the study; RLK analyzed the data and wrote the manuscript, JPS and CL generated the B6.*Cg-Tyr*$^{c\text{-}2J}$ *Hr*^{hr}/J mice and provided editorial support for the manuscript; RLK, ED-Y and DH performed the research.

Citations

1. Benavides F, et al. The hairless mouse in skin research. Journal of Dermatological Science. 2009; 53(1):10–18. [PubMed: 18938063]
2. Aubin-Houzelstein G, Panthier JJ. The Patchwork Mouse Phenotype: Implication for Melanocyte Replacement in the Hair Follicle. Pigment Cell Research. 1999; 12(3):181–186. [PubMed: 10385914]

3. Plikus MV, Chuong CM. Complex hair cycle domain patterns and regenerative hair waves in living rodents. The Journal of investigative dermatology. 2008; 128(5):1071–1080. [PubMed: 18094733]
4. Cachon-Gonzalez MB, et al. Structure and expression of the hairless gene of mice. Proceedings of the National Academy of Sciences. 1994; 91(16):7717–7721.
5. Sontag Y, et al. Time and Dose Dependence of Acceptance of UV-lnduced Syngeneic Tumor Implants in Chronically UV-Exposed Hairless Mice. Photochemistry and Photobiology. 1997; 65(2): 342–346. [PubMed: 9066309]
6. Afaq F, Ahmad N, Mukhtar H. Suppression of UVB-induced phosphorylation of mitogen-activated protein kinases and nuclear factor kappa B by green tea polyphenol in SKH-1 hairless mice. Oncogene. 2003; 22(58):9254–9264. [PubMed: 14681684]
7. Adhami VM, Afaq F, Ahmad N. Suppression of Ultraviolet B Exposure-Mediated Activation of NF-κB in Normal Human Keratinocytes by Resveratrol. Neoplasia. 2003; 5(1):74–82. [PubMed: 12659672]
8. Anwar A, et al. Photoprotective Effects of Bucillamine Against UV-induced Damage in an SKH-1 Hairless Mouse Model†. Photochemistry and Photobiology. 2008; 84(2):477–483. [PubMed: 18266821]
9. Wulff BC, et al. Celecoxib reduces the effects of acute and chronic UVB exposure in mice treated with therapeutically relevant immunosuppressive drugs. International Journal of Cancer. 2010; 126(1):11–18. [PubMed: 19609953]
10. Frijhoff AFW, et al. UVB-induced mutagenesis in hairless λlacZ-transgenic mice. Environ Mol Mutagenesis. 1997; 29(2):136–142.
11. Fischer SM, et al. Cyclooxygenase-2 expression is critical for chronic UV-induced murine skin carcinogenesis. Molecular Carcinogenesis. 2007; 46(5):363–71. [PubMed: 17219415]
12. Brouxhon S, et al. Deletion of prostaglandin E_2 EP_2 receptor protects against ultraviolet-induced carcinogenesis, but increases tumor aggressiveness. J Invest Dermatol. 2007; 127(2):439–46. [PubMed: 16977324]
13. Sahu RP, et al. Mice lacking epidermal PPARγ exhibit a marked augmentation in photocarcinogenesis associated with increased UVB-induced apoptosis, inflammation and barrier dysfunction. Int J Cancer. 2012; 131:E1055–E1066. [PubMed: 22467332]
14. Pentland AP, et al. Cyclooxygenase-1 deletion enhances apoptosis but does not protect against ultraviolet light-induced tumors. Cancer Research. 2004; 64(16):5587–91. [PubMed: 15313895]
15. Perez C, et al. SKHIN/Sprd, a new genetically defined inbred hairless mouse strain for UV-induced skin carcinogenesis studies. Experimental Dermatology. 2012; 21(3):217–220. [PubMed: 22379968]
16. EISENHOFER G, et al. Tyrosinase: a developmentally specific major determinant of peripheral dopamine. The FASEB Journal. 2003; 17(10):1248–1255. [PubMed: 12832289]
17. Klaus SN, Winkelmann RK. Pigment Changes Induced in Hairless Mice by Dimethylbenzanthracene1. The Journal of Investigative Dermatology. 1965; 45(3):160–167. [PubMed: 5829531]
18. Nair X, Tramposch KM. UVB-Induced Pigmentation in Hairless Mice as an in vivo Assay for Topical Skin-Depigmenting Activity. Skin Pharmacology and Physiology. 1989; 2(4):187–197.
19. Burd, Christin E., et al. Monitoring Tumorigenesis and Senescence In Vivo with a p16INK4a-Luciferase Model. Cell. 2013; 152(1–2):340–351. [PubMed: 23332765]
20. Schaffer BS, et al. Immune Competency of a Hairless Mouse Strain for Improved Preclinical Studies in Genetically-Engineered Mice. Molecular cancer therapeutics. 2010; 9(8):2354–2364. [PubMed: 20663932]
21. Konger R, et al. Spatiotemporal assessments of dermal hyperemia enable accurate prediction of experimental cutaneous carcinogenesis as well as chemopreventive activity. Cancer Res. 2013; 73:150–159. [PubMed: 23108146]
22. Liu L, et al. Hairless is a histone H3K9 demethylase. The FASEB Journal. 2014; 28(4):1534–1542. [PubMed: 24334705]
23. Kumpf S, et al. Hairless promotes PPAR expression and is required for white adipogenesis. EMBO Reports. 2012; 13(11):1012–20. [PubMed: 22964757]

24. Beaudoin GM 3rd, et al. Hairless triggers reactivation of hair growth by promoting Wnt signaling. Proceedings of the National Academy of Sciences of the United States of America. 2005; 102(41): 14653–8. [PubMed: 16195376]
25. Kim H, et al. Loss of hairless confers susceptibility to UVB-induced tumorigenesis via disruption of NF-kappaB signaling. PLoS ONE [Electronic Resource]. 2012; 7(6):e39691.
26. Ahmed MS, et al. Identification of novel mutation in the HR gene responsible for atrichia with papular lesions in a Pakistani family. Journal of Dermatology. 2013; 40(11):927–8. [PubMed: 24111842]
27. Azeem Z, et al. Congenital atrichia with papular lesions resulting from novel mutations in human hairless gene in four consanguineous families. Journal of Dermatology. 2011; 38(8):755–60. [PubMed: 21919222]
28. Sundberg, JP.; Dunstan, RW.; Compton, JG. Hairless Mouse, HRS/J hr/hr. In: Jones, TC.; Mohr, U.; Hunt, RD., editors. Integument and Mammary Glands. Springer-Verlag; Berlin Heidelberg: 1989.
29. Liu Y, et al. Molecular Basis for Hair Loss in Mice Carrying a Novel Nonsense Mutation (Hrrh-R) in the Hairless Gene (Hr). Veterinary Pathology Online. 2010; 47(1):167–176.
30. Berton TR, Pavone A, Fischer SM. Ultraviolet-B irradiation alters the cell cycle machinery in murine epidermis in vivo. Journal of Investigative Dermatology. 2001; 117(5):1171–8. [PubMed: 11710929]
31. Menter JM, et al. Dose-response of chronic ultraviolet exposure on epidermal forward scattering-absorption in SK-1 hairless mouse skin. Photochemistry and Photobiology. 1992; 55(5):705–712. [PubMed: 1528984]
32. Donnelly HT. Oxygen consumption, activity and body fat in normal and hairless mice. Laboratory Animals. 1982; 16:167–171. [PubMed: 7078063]
33. Chase HB, Montagna W, Malone JD. Changes in the skin in relation to the hair growth cycle. Anatomical Record. 1953; 116(1):75–81. [PubMed: 13050993]
34. Rodriguez-Burford C, et al. Selective Cyclooxygenase-2 Inhibition Produces Heterogeneous Erythema Response to Ultraviolet Irradiation. J Investig Dermatol. 2005; 125(6):1317–1320. [PubMed: 16354205]
35. Cole CA, et al. Comparison of action spectra for acute cutaneous responses to ultraviolet radiation: man and albion hairless mouse. Photochemistry and Photobiology. 1983; 37(6):623–631. [PubMed: 6611669]
36. Tripp CS, et al. Epidermal COX-2 induction following ultraviolet irradiation: suggested mechanism for the role of COX-2 inhibition in photoprotection. J Invest Dermatol. 2003; 121(4): 853–61. [PubMed: 14632205]
37. Gibbs NK, et al. The phototumorigenic potential of broad-band (270–350 nm) and narrow-band (311–313 nm) phototherapy sources cannot be predicted by their edematogenic potential in hairless mouse skin. Journal of Investigative Dermatology. 1995; 104(3):359–63. [PubMed: 7861002]
38. Dornelles S, Goldim J, Cestarl T. Determination of the Minimal Erythema Dose and Colorimetric Measurements as Indicators of Skin Sensitivity to UV-B Radiation¶. Photochemistry and Photobiology. 2004; 79(6):540–544. [PubMed: 15291306]
39. Agar NS, et al. The Basal Layer in Human Squamous Tumors Harbors More UVA Than UVB Fingerprint Mutations: A Role for UVA in Human Skin Carcinogenesis. Proceedings of the National Academy of Sciences of the United States of America. 2004; 101(14):4954–4959. [PubMed: 15041750]
40. Stoye JP, et al. Role of endogenous retroviruses as mutagens: The hairless mutation of mice. Cell. 1988; 54(3):383–391. [PubMed: 2840205]

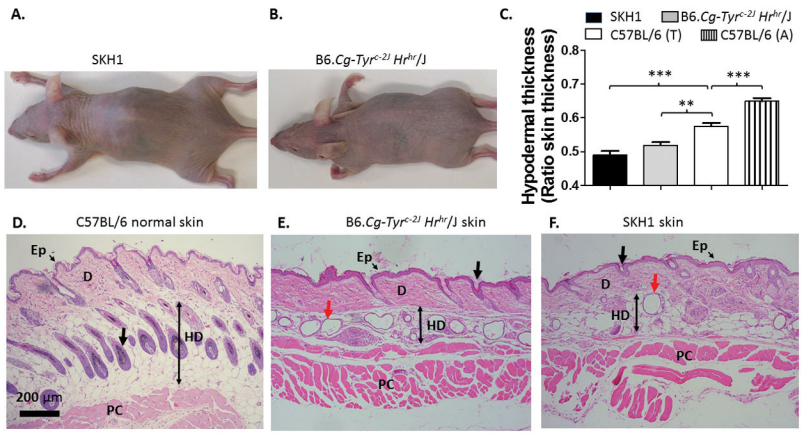

Figure 1. B6.*Cg-Tyr*$^{c\text{-}2J}$ *Hr*^{hr}/J phenotype relative to SKH1 mice

A & B) An SKH1 mouse is shown in relative to the smaller, but otherwise indistinguishable C57BL/6$^{Hr:Tyr-/-}$ mouse. C). The thickness of the hypodermis was measured as a ratio of the skin thickness (Hypodermis + dermis + epidermis, not including the panniculus carnosus). The mean and SEM of 5 random measurements in n=6–8 different sections from each mouse was measured. For wildtype C57BL/6 mice, measurements were done both during the telogen [T] and anagen [A] phase of the hair cycle. D–F). Histology of WT C57BL/6 mice during the mature anagen phase of hair growth (D), B6.*Cg-Tyr*$^{c\text{-}2J}$ *Hr*^{hr}/J mouse skin (E), and SKH1 mouse skin (F). The skin exhibits a thin epidermis (Ep) overlying a collagen dense dermis (D) and numerous hair follicles (black arrows) extending into the hypodermis (HD), but fail to enter the panniculus carnosus (PC). Hairless, albino skin is shown for B6.Cg-*Tyr*$^{c\text{-}2J}$ *Hr*^{hr}/J (lower middle panel) and SKH1 mice (lower right panel). The skin of both hairless mouse lines show similar histologic features, including a thickened epidermis with utricular pouches (black arrows), and the presence of cystic structures (red arrows) within a much thinner hypodermis.

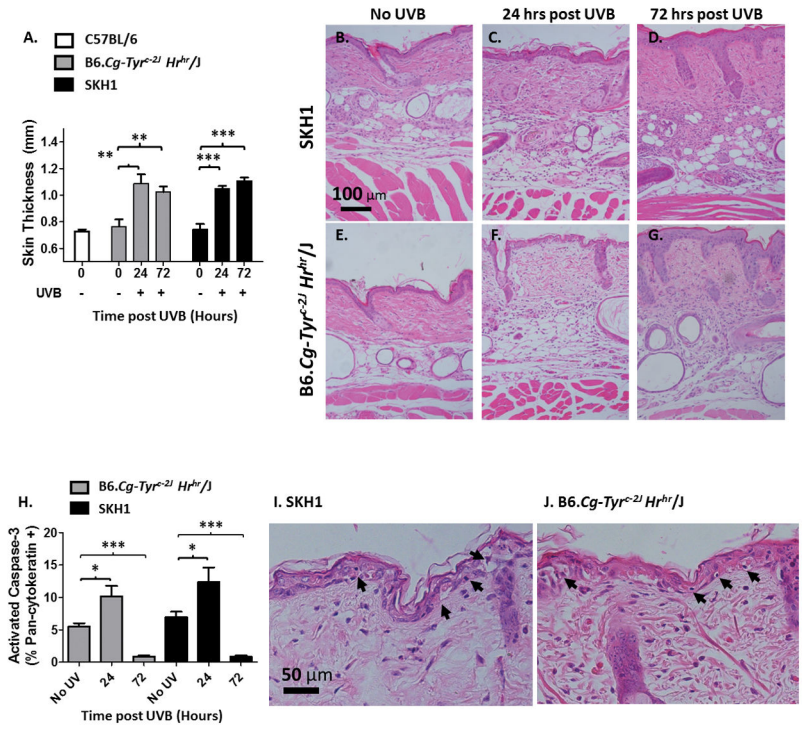

Figure 2. B6.*Cg-Tyr*$^{c-2J}$ *Hr*^{hr}/J and SKH1 mice exhibit similar edema and apoptotic responses to an acute UVB exposure

A) B6.*Cg-Tyr*$^{c-2J}$ *Hr*^{hr}/J and SKH1 mice were treated with 1500 J/m^2 of UVB, then euthanized 24 and 72 hours later. The dorsal UVB-treated skin was excised and the skin thickness was measured. For comparative purposes, the skin thickness of non-UVB treated C57BL/6 mice is also depicted. **, p<0.01; ***, p<0.001 (2-tailed *t*-test: n=4–6 mice per experimental group). B–G) Representative 200x photomicrographs of hematoxylin & eosin stained sections of SKH1 (B–D) and B6.*Cg-Tyr*$^{c-2J}$ *Hr*^{hr}/J (E–G) mice prior to UVB (B & E), 24 hours after UVB (C & F) and 72 hours post UVB (D & G). Epidermal disruption and increased dermal and hypodermal thickness are noted at 24 hours in both SKH1 and B6.*Cg-Tyr*$^{c-2J}$ *Hr*^{hr}/J mice. In addition, both groups of mice show similar degrees of epidermal hyperplasia and dermal/hypodermal inflammatory cell infiltrates at 24 hours & 72 hours post UVB. H) Mice were treated with 1500 J/m^2 of UVB and euthanized at 24 and 72 hours after UVB treatment. Immunofluorescent staining for pan-cytokeratin (pan-CK) and activated caspase-3 (CASP3) was then performed. Quantitation of apoptotic epidermal cells (pan-CK$^+$CASP3$^+$ cells) was performed by tissue cytometry. Relative to non-irradiated controls, both UVB treated mouse strains showed a similar increase in pan-CK$^+$CASP3$^+$ cells at 24 hours and a similar reduction in pan-CK$^+$CASP3$^+$ cells at 72 hours (*, p<0.05; ***, *p*<0.001; 2-tailed *t*-test. n=5–8/group). I & J) Representative photomicrograph (400x) of hematoxylin & eosin stained SKH1 skin (I) or B6.*Cg-Tyr*$^{c-2J}$ *Hr*^{hr}/J (J) skin at 24 hours post-UVB treatment. Both SKH1 and B6.*Cg-Tyr*$^{c-2J}$ *Hr*^{hr}/J epidermis shows marked epidermal disruption. Typical “sunburn” cytotoxic changes include the presence of multiple apoptotic cells marked by pyknotic nuclei, vacuolization, and eosinophilic cytoplasm (arrows).

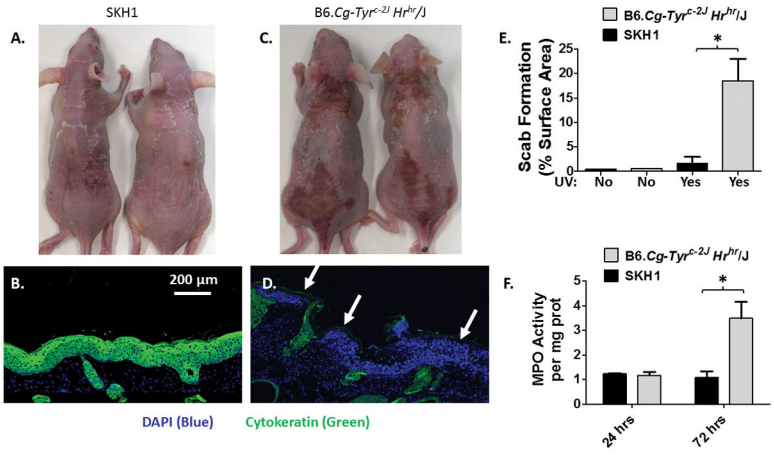

Figure 3. The delayed sunburn reaction and inflammation is augmented in B6.*Cg-Tyr*$^{c\text{-}2J}$ *Hr*^{hr}/J mice relative to SKH1 mice

Mice treated with a single 1500 J/m^2 UVB dose were observed to have peeling skin, erythema, and epidermal erosions with scab formation at 72 hours post-UVB. However, the degree of erosion and scab formation was increased in B6.*Cg-Tyr*$^{c\text{-}2J}$ *Hr*^{hr}/J mice relative to SKH1 mice by gross observation (A & C), and quantitation of scab formation as a percent of the dorsal surface area (E). In the immunofluorescence images seen in B & D, SKH1 epidermis is intact as assessed by pan-cytokeratin staining. In contrast, erosion of the epidermis is seen as loss of pan-CK$^+$ cells in the B6.*Cg-Tyr*$^{c\text{-}2J}$ *Hr*^{hr}/J mice (D). In contrast, the eroded epidermis is replaced by DAPI$^+$pan-CK$^-$ inflammatory cells within the scab (arrows in D). F). Myeloperoxidase activity is shown from skin preparations of UVB-treated B6.*Cg-Tyr*$^{c\text{-}2J}$ *Hr*^{hr}/J and SKH1 mice. A significant increase in cutaneous leukocyte myeloperoxidase activity was observed in B6.*Cg-Tyr*$^{c\text{-}2J}$ *Hr*^{hr}/J mice at 72 hours post-UVB relative to their UVB-treated SKH1 counterparts.

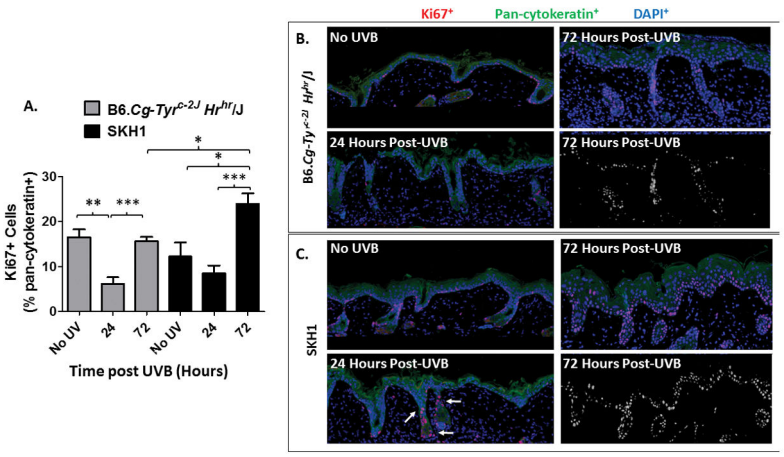

Figure 4. UVB-induced proliferative responses differ between SKH1 and B6.*Cg-Tyr*$^{c-2J}$ *Hr*^{hr}/J mice

A) Mice were treated with or without a single 1500 J/m^2 UVB dose. UVB treated mice were euthanized at 24 and 72 hours post UVB. Immunofluorescence was performed using antibodies against the proliferation marker Ki67 and the epidermal marker pan-cytokeratin (pan-CK). Ki67$^+$pan-CK$^+$ cells were quantitated by tissue cytometry. Results shown are expressed as the mean and SEM (n=5–6/group). *, p<0.05; **, p<0.01; ***, p<0.001; 2-tailed t-test. (B & C) Representative photomicrographs of Ki67 immunofluorescent staining of (A) B6.*Cg-Tyr*$^{c-2J}$ *Hr*^{hr}/J mice and (B) SKH1 mice was performed: Ki67 (red), pan-cytokeratin (pan-CK; Green), DAPI (Blue). Ki67$^+$ cells are observed in the basal layer of non-UVB treated B6.*Cg-Tyr*$^{c-2J}$ *Hr*^{hr}/J and SKH-1 mice (upper left panels in (B) & (C)). When examined 24 hours after UVB treatment, Ki67$^+$ cells are largely absent in the interfollicular epidermis of UVB-treated B6.*Cg-Tyr*$^{c-2J}$ *Hr*^{hr}/J and SKH1 mice (Lower left panels in (B) & (C)). However, SKH1 mice exhibit a less pronounced decrease in Ki67$^+$ cells, particular in keratinocytes within the deeper portions of hair follicles (See white arrows in (C)). At 72 hours (upper and lower panels on right in (B) & (C)), Ki67$^+$ epidermal cells are increased in SKH1 mice relative to B6.*Cg-Tyr*$^{c-2J}$ *Hr*^{hr}/J mice. The right upper panels in (B) & (C) represent merged images (Ki67$^+$pan-CK$^+$DAPI$^+$) while the right lower panels represent monochrome images of Ki67$^+$ cells only.